Kareinen *et al. Earth, Planets and Space* (2017) 69:16
DOI 10.1186/s40623-017-0601-y

Earth, Planets and Space

LETTER

Open Access

Identifying optimal tag-along station locations for improving VLBI Intensive sessions

Niko Kareinen*, Grzegorz Klopotek, Thomas Hobiger and Rüdiger Haas

Abstract

Very Long Baseline Interferometry (VLBI) is a unique space-geodetic technique capable of direct observation of the Earth's phase of rotation, namely Universal Time (UT1). The International VLBI Service for Geodesy and Astrometry (IVS) conducts daily 1-h Intensive VLBI sessions to determine rapid variations in the difference between UT1 and Coordinated Universal Time (UTC). The main objective of the Intensive sessions is to provide timely UT1–UTC estimates. These estimates are especially crucial for Global Navigation Satellite Systems (GNSS). The monitoring of rapid variations in Earth rotation also provides insight into various geophysical phenomena. There is an ongoing effort to improve the quality of the UT1–UTC estimates from single-baseline Intensive sessions to realise the expected accuracy and to bring them to a better agreement with the 24-h VLBI sessions. In this paper, we investigate the possibility to improve the Intensives by including a third station in tag-along mode to these regularly observed sessions. The impact of the additional station is studied via extensive simulations using the c5++ analysis software. The location of the station is varied within a predetermined grid. Based on actual Intensive session schedules, a set of simulated observations are generated for the two original stations and each grid point. These simulated data are used to estimate UT1–UTC for every Intensive session scheduled during the year 2014 on the Kokee–Wettzell and Tsukuba–Wettzell baselines, with the addition of a third station. We find that in tag-along mode when a third station is added to the schedule we can identify areas where the UT1–UTC estimates are improved up to 67% w.r.t. the original single-baseline network. There are multiple operational VLBI stations in these areas, which could with little effort be included in a tag-along mode to the currently scheduled Intensive sessions, thus providing the possibility to improve the UT1–UTC estimates by extending the observation network.

Keywords: VLBI, VGOS, UT1, Earth rotation, Intensives

Background

Very Long Baseline Interferometry (VLBI) (Sovers et al. 1998) is the only space-geodetic technique capable of direct observations of UT1, the Earth's angle of rotation about the Celestial Intermediate Pole (CIP) axis. Geodetic VLBI observations provide an estimate for the difference between UT1 and Coordinated Universal Time (UTC), UT1–UTC.

The International VLBI Service for Geodesy and Astrometry (IVS) (Nothnagel et al. 2016) coordinates 1-h-long Intensive VLBI sessions for the purpose of providing a daily UT1–UTC estimate. These sessions are essential in providing updated UT1 estimates for the Global Navigation Satellite Systems (GNSS). Currently, three types of Intensive sessions are being conducted. INT1 sessions are observed on a baseline between Kokee Park (Hawaii, USA) and Wettzell (Bad Kötzting, Germany) from Monday to Friday, starting at 18:30 UTC (18:45 on Fridays). INT2 sessions are observed on a baseline between Wettzell and Tsukuba (Japan) on Saturdays and Sundays at 7:30 UTC. To fill the gap between the INT2 session on Sunday and INT1 session on Monday, one INT3 session is observed weekly on Mondays at 7:00 UTC between Tsukuba, Wettzell, and Ny-Ålesund (Norway, Spitsbergen).

Since the beginning of the Intensive observing series, efforts have been made to improve the performance of the Intensive sessions. Many efforts have been directed

*Correspondence: niko.kareinen@chalmers.se
Department of Earth and Space Sciences, Chalmers University of Technology, Onsala Space Observatory, 439 92 Onsala, Sweden

© The Author(s) 2017. This article is distributed under the terms of the Creative Commons Attribution 4.0 International License (http://creativecommons.org/licenses/by/4.0/), which permits unrestricted use, distribution, and reproduction in any medium, provided you give appropriate credit to the original author(s) and the source, provide a link to the Creative Commons license, and indicate if changes were made.

towards scheduling-based approaches. For example, Gipson and Baver (2016) investigated the benefits of selecting sources from a pool of all visible sources versus a limited list of strong sources. Uunila et al. (2012) looked at classifying sessions based on the distributions of the observed sources. Leek et al. (2015) studied the use of impact factors to optimise the observing geometry. This approach was also applied to scheduling Intensive sessions for a twin-telescope system at Wettzell. The impact of longer session duration of 2 h for the Intensive sessions was investigated in Artz et al. (2012). This research showed that a twofold increase in session duration reduces the formal errors by a factor of $\sqrt{2}$.

These previous studies have primarily addressed geometry and session duration. Other important deficiencies of the current Intensive sessions are the limited number of observations (20–40) and the lack of redundancy of the observations. The INT1 and INT2 sessions are observed on extended East-West baselines using two telescopes. Occasionally, these sessions are joined by one or two additional stations. In this paper, by carrying out extensive simulations, we look into the improvement of the UT1 accuracy which can be obtained by adding a third station to the observing geometry in a tag-along mode. When a station is added in tag-along mode to a VLBI session, this implies that this station should observe as many as possible of the scheduled sources, although the station was not included in the scheduling optimisation process (e.g. sky coverage, number of observations). Thus, tag-along observations can be performed dynamically, provided that a station becomes available.

We concentrate on the INT1 and INT2 sessions scheduled for the year 2014 (230 and 102 sessions, respectively). We define a grid of possible station locations for the third station based on visibilities of the scheduled sources throughout the year. For each grid point, we compute the UT1–UTC w.r.t. IERS C04 08 (Bizouard and Gambis 2011) value. By comparing these results to corresponding UT1–UTC accuracies from the original observing network, we calculate the improvement factor gained by tagging along the third station. Here, by corresponding UT1–UTC accuracies we mean the reference UT1–UTC values computed from simulated observations using the real schedules. The UT1–UTC accuracy of real, observed, and analysed IVS Intensive sessions for select time periods and different sessions types have been presented in previous literature. For example, Baver et al. (2012) report an UT1–TAI RMS difference to C04 of $\sim$ 25 μs for INT1 during the year 2011. Moreover, as given by Malkin (2013), for INT1 (2005–2011), INT2 (2005–2011), and INT3 (2007–2011) the UT1–UTC WRMS w.r.t C04 was 18.0, 9.9, and 18.5 μs, respectively.

This tag-along approach has a potential importance for the upcoming VLBI Global Observing System (VGOS), which aims at continuous monitoring of the EOPs. Currently, when the VLBI observations are scheduled, the participating stations are known a priori. When the observations are done in a continuous mode, stations could become available or unavailable at any given time. This dynamical aspect needs to be taken into account in the scheduling for VGOS observations. Consequently, optimised schedules are only available for the stations that participate regularly and reliably in a given session type. Naturally, rescheduling the observations on-the-fly as stations enter or leave the pool of available sites would yield better results in terms of the optimisation conditions. The concept of dynamical scheduling has been investigated by Lovell et al. (2014). However, this type of dynamic scheduling is still in the future. Furthermore, the observation schedules are optimised to determine a set of target parameters. By tagging along one does not need to interfere with the original purpose of the schedule. This gives prospective stations flexibility in opting in/out in an observing session.

In the context of prescheduled observations, tagging along extra stations to the standard schedules and adding new stations dynamically to an observation schedule are comparable situations. This makes it possible to apply the knowledge about the impact of the simulated third station to a situation where dynamic scheduling is needed.

Methods

The effect of adding a third VLBI telescope to the INT1 and INT2 observing networks in terms of UT1–UTC accuracy was investigated through extensive simulations. The analysis was performed using the c5++ analysis software (Hobiger et al. 2010). The main data sets used consist of VEX files (Whitney et al. 2002) for the INT1 and INT2 sessions observed during 2014. When the observation schedules were initially created for the Intensive sessions, the sources were selected following criteria that optimise the source selection for the original observing network. In the simulations the third station was added to the observing schedule in a tag-along mode. This means that the observed sources were taken from the original schedules for the respective INT1 and INT2 sessions. The third station observes alongside the original observation network if the sources are visible and above the elevation cut-off limit at its location. It is assumed that the third station has sufficient slewing capability and sensitivity to observe the scheduled sources. It is obvious that the simulations do not reflect an optimised observing strategy for the proposed three-station network. Nevertheless, one can expect an improvement by just tagging along with an existing schedule.

The initial grid spanned all locations from 0 to 358° in longitude and −90 to 90 in latitude, in 2° steps. In order to remove grid points from which the observed sources are not visible for the third station to sufficient degree within an observing session, an initial grid-trimming run was carried out. We determined for both INT1 and INT2 a latitude–longitude grid such that the third station is included in at least 40, 60, and 80% of the scheduled scans. For each scan that includes the third station the number of observations increase from 1 to 3. These percentages define three inclusion levels, 0.4, 0.6, and 0.8, which are referred to as the Tag-Along Factors (TAFs). This resulted in three grids of differing minimum TAF values for both session types. If for any session during 2014 the TAF was below the target level, the location was permanently removed from the grid. This guarantees that at all the remaining grid points at least 40% of the scans can be tagged along throughout the year. The resulting two grids for INT1 and INT2 sessions, respectively, were used as the basis for possible locations of the third station in the network. The common points in the INT1 and INT2 grids form a third grid, which can be understood as the intersecting set INT1 ∩ INT2. The extent of the areas with 0.4, 0.6, and 0.8 TAF for the three grids is illustrated in Fig. 1. The areas are annotated with letters A (TAF 0.8), B (TAF 0.6), and C (TAF 0.4), which are used to refer to the respective areas throughout this paper. The areas are inclusive—area A is included in area B, and area B is included in area C.

Simulated observations in c5++

The c5++ analysis software was used for the analysis in this study. In order to compute the theoretical delays, c5++ follows the latest International Earth Rotation and Reference Systems Service (IERS) conventions (Petit and Luzum 2010). The software package was extended with the capability to simulate observations and was used to run extensive Monte Carlo simulations for each INT1 and INT2 session scheduled during the year 2014. A simulated observation on a baseline includes contributions from the station clocks, local tropospheres, and a baseline-dependent noise component. The station clocks were modelled as integrated random walk processes with the clock stability per time unit as a tunable parameter. The troposphere was modelled using the Kolmogorov turbulence model (Treuhaft and Lanyi 1987) following the approach of Nilsson and Haas (2010). The observation noise component was simulated as baseline-dependent in order to be consistent with the set-up used in the simulations that were carried out during the studies of the requirements and capabilities of VGOS (Petrachenko et al. 2009).

In general, the atmospheric turbulence is simulated using three parameters: refractive index structure constant C_n, troposphere height H, and wind speed. The C_n values for different VLBI stations are provided in Petrachenko et al. (2009). For the VLBI stations relevant to INT1 and INT2 sessions, Kokee, Wettzell, and Tsukuba, these values were directly available from the tabulated values. To provide structure constant values for the third station at an arbitrary point, C_n values were interpolated on a $2° \times 2°$ rectangular grid. The interpolation was done using the *greenspline* function (Wessel 2009) of the Generic Mapping Tools (GMT) (Wessel et al. 2013). For the troposphere height and wind constant values were used.

To estimate the relative effect of adding the third station to the INT1 and INT2 observing geometries, reference UT1–UTC Weighted Root Mean Square (WRMS) values were computed for both session types. The station clocks and the baseline-dependent observation noise were simulated with identical parameters for all stations. The reference values for the INT1 and INT2 were computed by generating 500 UT1–UTC estimates for each session and from these computing one yearly reference WRMS value for the INT1 and INT2 sessions, respectively.

For the simulations which included the third station we used the same simulation parameters for the station clocks, baseline-dependent observation noise, troposphere height, and wind speed as in the reference computations. The only varying quantity in generating the simulated observations for the extended network was the location-dependent structure constant C_n of the third station. In order to keep the computational time manageable, each simulated network configuration (i.e. grid point) was computed 20 times. Thus, for each session we obtained a UT1–UTC WRMS value for every grid point, computed from the 20 iterations, which were subsequently averaged to a yearly value. Given the number of INT1 and INT2 sessions and the grid sizes, this resulted in more than 27 million and 11 million simulated observations, respectively.

For the troposphere height H a constant value of 2 km was used for both the actual stations and the additional third station. Similarly, a constant wind speed of 5 m/s (North and East component) was applied for all stations. The station clocks were characterised with a stability of 10^{-14} @ 50 min. The baseline-dependent observation noise was set to 0.01 m (33 ps) for all baselines. The station-dependent C_n values in units of 10^{-7} $m^{-1/3}$ were 0.938080 at Wettzell, 2.297883 at Kokee, and 1.445493 at Tsukuba.

To compute the target parameter, UT1–UTC, the sessions were processed following the standard set-up used in operational INT analysis. The estimated parameters were: station clocks (excluding the reference clock)

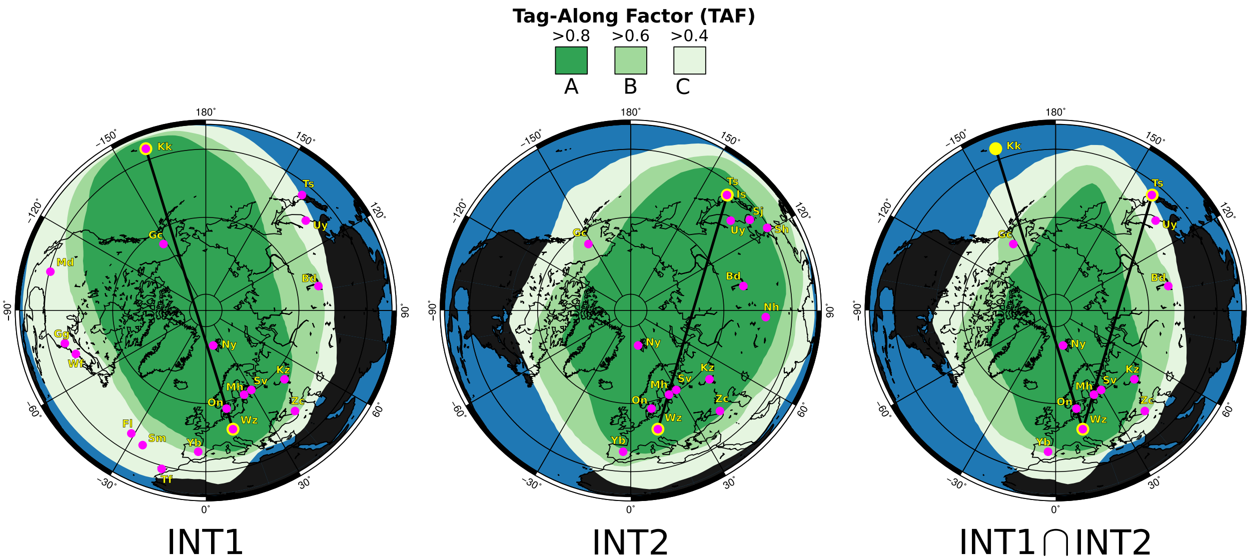

Fig. 1 Maps of the extent of the A (TAF > 0.8), B (TAF > 0.6), and C (TAF > 0.4) grids for the INT1 (*left*), INT2 (*middle*), and INT1 ∩ INT2 (*right*). The VGOS stations are annotated by their two-letter station codes. See Table 2 for the corresponding site names for the abbreviated names

modelled as quadratic polynomials (three parameters per clock), the troposphere with one Zenith Wet Delay (ZWD) per station, and the target parameter UT1–UTC. For the a priori EOP values we used the IERS C04 08 series (Bizouard and Gambis 2011). Thus, the estimated UT1–UTC are given w.r.t. these a prioris. In a real-life scenario the C04 series is not yet available at the time of operational analysis of the INT sessions. Instead, predicted a priori EOP values are used. This means that the scatter of the UT1–UTC values derived from the simulated observations is too optimistic when comparing with the UT1–UTC obtained from the analysis of real INT sessions. However, this is not an issue when investigating the performance of the three-station network, since we always compare our values to the simulated reference values, which also use the same series as a prioris.

Results

The relative improvement in UT1–UTC accuracy gained by adding a third station in tag-along mode to the INT1 and INT2 observing networks was investigated in spatial sense by varying the location of the third station on the grids described in the previous section. The simulated reference UT1–UTC WRMS values for standard INT1 and INT2 observing networks for the year 2014 were 15.43 and 12.03 µs, respectively.

To express the relative improvement in UT1–UTC WRMS given by adding a third station, we define a WRMS ratio parameter

$$\beta = \frac{\mathrm{WRMS}_{3\,\mathrm{stations}}}{\mathrm{WRMS}_{2\,\mathrm{stations}}}, \quad (1)$$

where $\mathrm{WRMS}_{2\,\mathrm{stations}}$ is the reference UT1–UTC WRMS obtained using the standard two-station networks of INT1 and INT2 sessions. The numerator, $\mathrm{WRMS}_{3\,\mathrm{stations}}$, is the UT1–UTC WRMS computed with the addition of the third station. This means values smaller than one indicate an improvement w.r.t. the reference solution.

When the individual grids for INT1 and INT2 are combined into one grid that contains all the mutual locations, we obtain three sets of points where the third station produces a TAF of at least 0.4, 0.6, and 0.8 in both session types. In the following these three grids will be referred to as INT1 grid, INT2 grid, and INT1 ∩ INT2 grid in the text.

The β-values for these three grids are illustrated in Fig. 2. From these maps we can see that both session types get the largest improvement when the third station is situated in North Pacific and Alaska regions. The β-values for the INT1 ∩ INT2 grid are averaged from the individual INT1 and INT2 grid values according to

$$\beta_{\mathrm{INT1} \cap \mathrm{INT2}} = \frac{\beta_{\mathrm{INT1}} + \beta_{\mathrm{INT2}}}{2}, \quad (2)$$

where β_{INT1} and β_{INT2} are the respective β-values for the INT1 and INT2 grids.

In general, the best area for the third station in terms of improved UT1–UTC accuracy spans from Alaska through the North Pacific to Eastern Siberia. In contrast to that, a third station in Northern Africa yields the lowest level of improvement.

The optimal locations (minimum β-value) for the third station in INT1, INT2, and the mutual grid are listed in

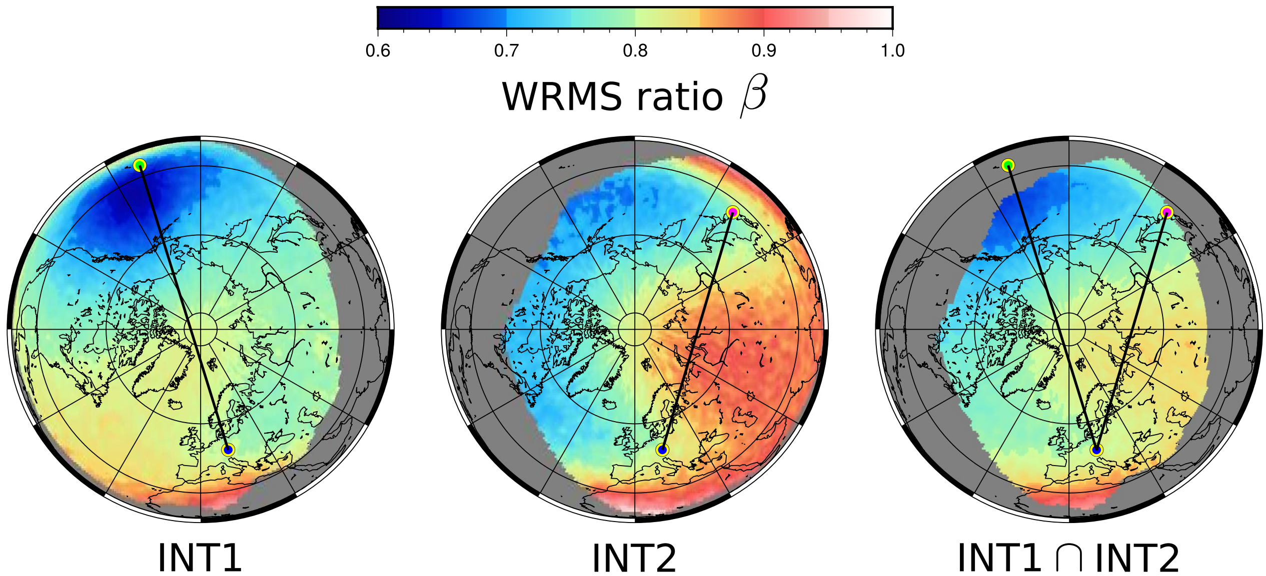

Fig. 2 Maps of β-values for INT1, INT2, and INT1 ∩ INT2. Each grid point corresponds to a β-value for the year 2014, which is obtained when the third station is located on that grid point (Kokee: *blue dot*, Wettzell: *green dot*, Tsukuba: *magenta dot*)

Table 1. The absolute values for the mean formal errors and WRMS for the UT1–UTC are depicted in Figs. 3 and 4. These maps illustrate that in general formal errors are too optimistic compared to the UT1–UTC residuals. The correlation between the areas with low UT1–UTC WRMS and mean formal error has large variation between the three grids. The respective Pearson correlation coefficients for the INT1, INT2, and the mutual grids are 0.34, 0.88, and 0.63. This indicates that especially with INT1 sessions, scheduling based only on formal errors may not provide optimal UT1–UTC accuracy. This can be attributed to the fact that troposphere correlations were implicitly imposed when generating the simulated observations, but the estimation algorithm does not take into account the correlations between the observations.

The asymmetric distribution of the WRMS values is driven by tropospheric turbulence, expressed by the C_n values, and the geometry of the three-station network. Considering that tropospheric turbulence increases towards the equator one would expect that tag-along sites located further North lead to less noisy observations and thus better UT1–UTC estimates. However, under the aspect of geometry, optimum UT1–UTC estimation would be achieved by maximising the length of the baseline projected to the equatorial plane, i.e. increasing the sensitivity of the network w.r.t. this Earth Orientation Parameter. Thus, the patterns of the β-values depicted in Fig. 2 can be understood accordingly. As for the INT1 sessions, extending the baseline South of Kokee or Wettzell does not lead to better UT1–UTC determination since any tag-along station would be placed in a location of high atmospheric turbulence. Putting a third station North of Wettzell helps with the UT1–UTC determination to some extent; however, the obtained geometry does not allow for significant improvements. On the contrary, the situation for Kokee, which is located approximately 27° closer to the equator, is different. Here, placing a site North of Kokee leads to less turbulence while still providing a geometry which improves UT1–UTC. Thus, the combination of both factors, turbulence and geometry, indicates an area of significant improvement North of Kokee. In a similar way one can interpret the pattern seen from the β-values of INT2, and however for this case, the non-symmetric orientation of the Tsukuba–Wettzell baseline has to be taken into account. Since both stations are not differing much in latitude, going North at any of the two stations helps to improve UT1–UTC. Paired with the impact of geometry a crescent-shaped pattern is identified as suitable area for tag-along sites. The lower mean UT1–UTC formal errors around Wettzell are due to lower atmospheric turbulence in that area.

The β-values from the three-station network simulations were within a range of 0.60–0.97, translating into improvements between 0.03 and 0.40. In order to assess the characteristics of the different levels of the improvements the values were divided into four categories—relative improvement between 0.0–0.1, 0.1–0.2, 0.2–0.3, and 0.3–0.4. Illustrated in Fig. 5 is the percentage of the

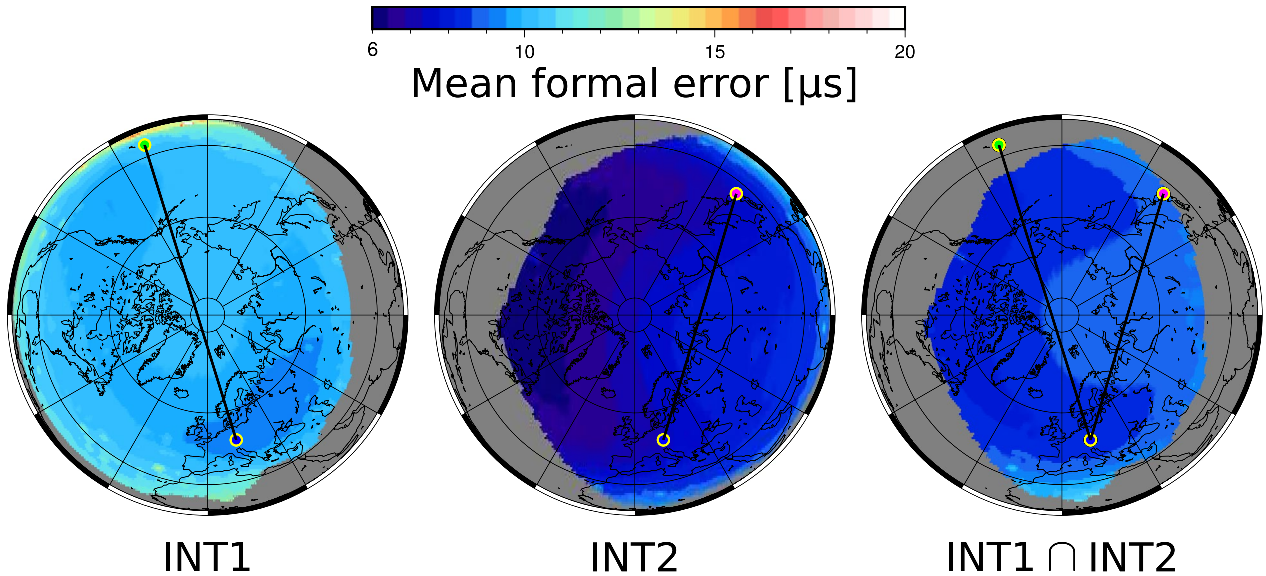

Fig. 3 Maps of UT1–UTC mean formal errors for INT1, INT2, and INT1 ∩ INT2. Each grid point corresponds to UT1–UTC mean formal error for the year 2014, which is obtained when the third station is located on that grid point (Kokee: *green dot*, Wettzell: *blue dot*, Tsukuba: *magenta dot*)

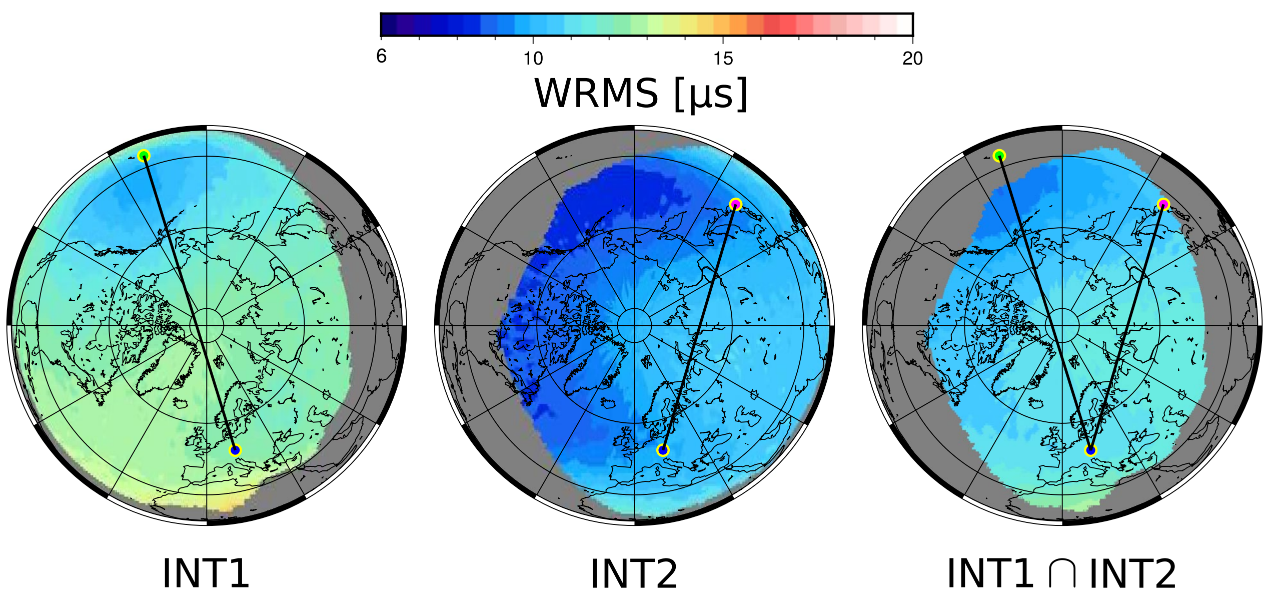

Fig. 4 Maps of UT1–UTC WRMS for INT1, INT2, and INT1 ∩ INT2. Each grid point corresponds to UT1–UTC WRMS for the year 2014, which is obtained when the third station is located on that grid point (Kokee: *green dot*, Wettzell: *blue dot*, Tsukuba: *magenta dot*)

grids points relative to the corresponding area (A, B, C) size for each improvement category. The majority of the grid points provide an improvement in the ranges of 0.1–0.2 and 0.2–0.3. For INT1 sessions there are also several grid points in the higher improvement category of 0.3–0.4. Generally, the higher TAF values with area A provide a similar level of improvement compared to the lower TAF values. This can be understood as areas with lower TAF might still provide an advantageous geometry even with less scans. Within the areas that provide an improvement of UT1–UTC there are currently multiple upcoming VGOS stations. Table 2 provides the stations that are located within areas A, B, and C for each session type.

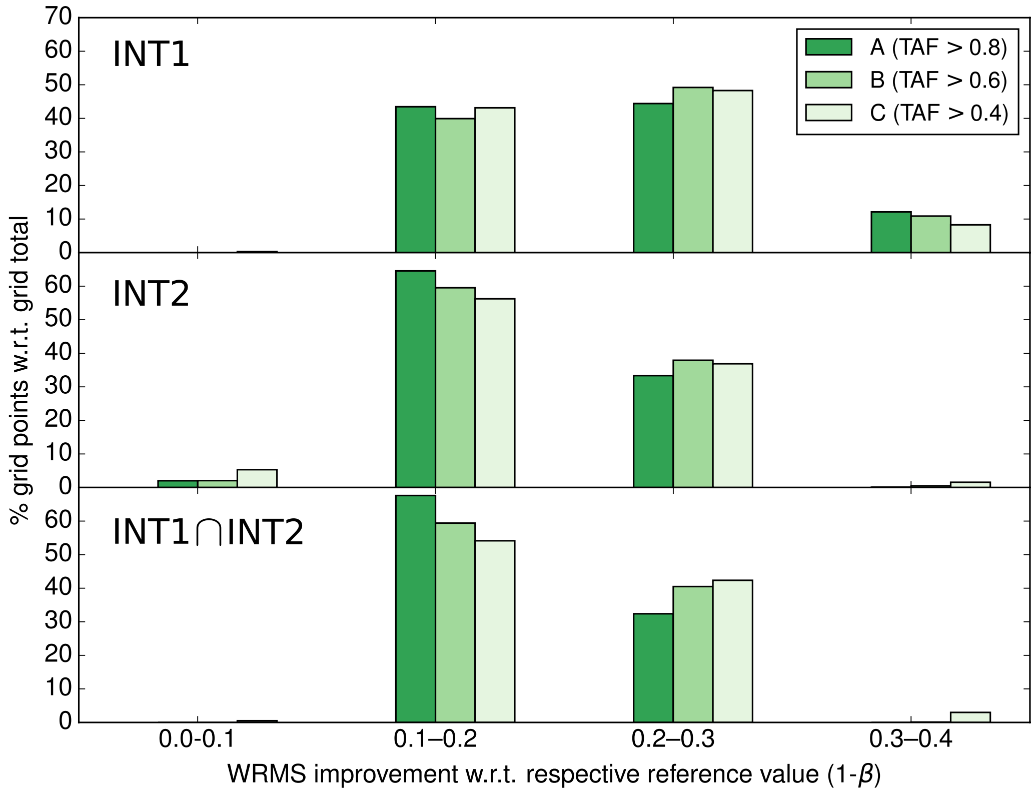

Fig. 5 Histograms illustrating the distribution of the grid points in areas *A*, *B*, and *C* into the relative improvement categories. *Each area* is scaled by their corresponding total size to yield the percentages. Shown are the histograms for INT1 (*top*), INT2 (*middle*), and INT1 ∩ INT2 (*bottom*)

Table 1 Minimum and maximum β-values and their locations for the three grids (INT1, INT2, and INT1 ∩ INT2)

	Min β	(Lat, Lon)	Max β	(Lat, Lon)
INT1, A	0.61	(39, 210)	0.85	(67, 312)
INT1, B	0.61	(39, 210)	0.87	(37, 16)
INT1, C	0.61	(39, 210)	0.94	(19, 4)
INT2, A	0.69	(53, 170)	0.93	(59, 72)
INT2, B	0.69	(49, 172)	0.93	(59, 72)
INT2, C	0.67	(43, 186)	0.97	(21, 356)
INT1 ∩ INT2, A	0.71	(53, 170)	0.86	(67, 54)
INT1 ∩ INT2, B	0.69	(51, 184)	0.87	(37, 18)
INT1 ∩ INT2, C	0.66	(43, 204)	0.94	(19, 4)

Conclusions

In this paper, we investigated the potential to improve UT1–UTC estimated from the INT1 and INT2 sessions by adding a third station to the existing observing network in a tag-along mode. The UT1–UTC estimated with a simulated three-station network have up to 40% smaller yearly WRMS compared to the simulated reference values. The largest improvement is obtained in an East-West sector that spans from Alaska over the North Pacific to the Eastern parts of Siberia. Overall, nearly at every point on the grid an improvement of at least 20–30% was obtained throughout the year in every scheduled INT1 and INT2 session. A particularly favourable zone for an additional station is found north of Kokee Park up to the Alaskan peninsula.

The improved UT1–UTC values were achieved by simply tagging along the third station to the observation network. It is viable that optimised scheduling could further improve the level of UT1–UTC accuracy that can be achieved with the three-station Intensive network. Simulations using the real INT3 schedules yielded a reference UT1–UTC w.r.t. C04 value of 10.8 µs. Concerning scheduling the tag-along mode offers an easy-to-implement solution for many existing stations. In total 12 of the upcoming VGOS stations are located within the mutual (INT1 ∩ INT2) grid. Half of these stations belong to the area A in terms of additional observed baselines.

One of the deficiencies of the current Intensive sessions is the limited number of observations (20–40). Second, the two-station network lacks redundancy and is thus more susceptible to lost scans. In contrast to increasing the observing time of the Intensive sessions from the 1-h duration, the three-station approach addresses

Table 2 A list of upcoming VGOS stations (Hase and Pedreros 2014) which are located within the area where the third station scheduled in a tag-along mode provides an improvement to the UT1–UTC estimated from the INT1 and INT2 sessions

	INT1		INT2		INT1 ∩ INT2	
	Area	β	Area	β	Area	β
Wettzell (VGOS) (Wz)	A	0.81	A	0.79	A	0.80
Onsala (On)	A	0.80	A	0.81	A	0.81
Metsähovi (Mh)	A	0.79	A	0.84	A	0.82
Ny-Ålesund (Ny)	A	0.81	A	0.83	A	0.82
Svetloe (Sv)	A	0.80	A	0.85	A	0.83
Kazan (Kz)	A	0.79	A	0.88	A	0.84
Gilmore Creek (Gc)	A	0.73	B	0.73	B	0.73
Badary (Bd)	B	0.79	A	0.86	B	0.82
Zelenchukskaya (Zc)	B	0.79	A	0.86	B	0.83
Ussuriysk (Uy)	C	0.77	A	0.79	C	0.78
Yebes (Yb)	C	0.83	B	0.83	C	0.83
Ishioka (Is)	–	–	A	0.77	–	–
Sejong (Sj)	–	–	A	0.80	–	–
Seshan (Sh)	–	–	A	0.83	–	–
Nanshan (Nh)	–	–	A	0.88	–	–
Kokee (VGOS) (Kk)	A	0.68	–	–	–	–
McDonald (Md)	C	0.77	–	–	–	–
Greenbelt (Gg)	C	0.81	–	–	–	–
Westford (Wf)	C	0.81	–	–	–	–
Flores (Fl)	C	0.84	–	–	–	–
Santa Maria (Sm)	C	0.84	–	–	–	–
Tenerife (Tf)	C	0.86	–	–	–	–

For each station the following attributes are listed: the grids (INT1, INT2, or INT1 ∩ INT2) in which the station is found and the corresponding areas (A, B, C) and an interpolated β-value of the UT1–UTC on the grid

in addition to the increased number of observations also the weaknesses in the observing geometry. Approaches to improve the performance of the INT sessions with an emphasis on near-real time applications have been studied in, e.g., Hobiger et al. (2010) and Kareinen et al. (2015). Similarly, the TAF and UT1–UTC WRMS maps are suitable for near-real time applications by providing a spatially dependent selection criteria for scheduling.

Based on the simulations carried out in this paper it is possible to indicate areas containing upcoming VGOS sites as well as currently operational VLBI stations where adding a third station in tag-along mode would improve the UT1–UTC accuracy of the Intensives. The results presented in this paper can also be seen as a complemental contribution to the Global Geodetic Observing System (GGOS) (Plag and Pearlman 2009), for which Otsubo et al. (2016) have studied how Satellite Laser Ranging (SLR) station networks can be extended and scheduled for optimum determination of geodetic target parameters. In this paper, we have investigated a similar extension scheme for the new VGOS sites. By concentrating on some of the most promising areas, further simulations with schedules optimised for the three-station configurations may provide even better insight on the optimal three-station network geometry. Continuous VGOS observations require a scheduling scheme which is able to respond to changes in the availability of the stations in the observing network. The simulated maps provide information about the spatial dependence of the increase in UT1–UTC accuracy that is gained with the third station. They provide a tool to aid in site selection when the VLBI observations are scheduled on-the-fly. This can be especially useful in the case where stations need to be scheduled dynamically, which is a likely scenario in continuous VGOS operations.

Abbreviations

CIP: Celestial Intermediate Pole; GGOS: Global Geodetic Observing System; GMT: Generic Mapping Tools; GNSS: Global Navigation Satellite Systems; IERS: International Earth Rotation and Reference Systems Service; IVS: International VLBI Service for Geodesy and Astrometry; SLR: Satellite Laser Ranging; TAF: Tag-Along Factor; UT1: Universal Time; UTC: Coordinated Universal Time; VGOS: VLBI Global Observing System; VLBI: Very Long Baseline Interferometry; WRMS: Weighted Root Mean Square; ZWD: Zenith Wet Delay.

Authors' contributions

NK performed all the data analysis, prepared the graphical material, and wrote the manuscript. GK wrote the simulation module for c5++. TH and RH supervised NK and helped to improve the manuscript. All authors read and approved the final manuscript.

Acknowlegements

We would like to thank Axel Nothnagel for our inspiring conversations, during which the initial idea for this study was formed. We would also like to acknowledge the IVS (Nothnagel et al. 2016) for providing the VEX files used in this study. Lastly, we want to thank the two anonymous reviewers for their constructive comments, which helped to improve this paper.

Competing interests

The authors declare that they have no competing interests.

Received: 13 October 2016 Accepted: 11 January 2017
Published online: 25 January 2017

References

Artz T, Leek J, Nothnagel A, Schumacher M (2012) VLBI intensive sessions revisited. In: Behrend D, Baver KD (eds) IVS 2012 general meeting proceedings "Launching the Next-Generation IVS Network", NASA/CP-2012-217504, pp 86–90

Baver K, Gipson J, Carter MS, Kingham K (2012) Assessment of the first use of the uniform sky strategy in scheduling the operational IVS-INT01 sessions. In: Behrend D, Baver KD (eds) IVS 2012 general meeting proceedings "Launching the Next-Generation IVS Network", NASA/CP-2012-217504, pp 251–255

Bizouard C, Gambis D (2011) IERS C04 08. https://hpiers.obspm.fr/iers/eop/eopc04/C04.guide.pdf, the combined solution C04 for Earth Orientation Parameters consistent with International Terrestrial Reference Frame 2008. Accessed 5 Jan 2017

Gipson J, Baver K (2016) Improvement of the IVS-INT01 sessions by source selection: development and evaluation of the maximal source strategy. J Geod 90(3):287–303. doi:10.1007/s00190-015-0873-6

Hase H, Pedreros F (2014) The most remote point method for the site selection of the future GGOS network. J Geod 88(10):989–1006. doi:10.1007/s00190-014-0731-y

Hobiger T, Otsubo T, Sekido M, Gotoh T, Kubooka T, Takiguchi H (2010) Fully automated VLBI analysis with c5++ for ultra-rapid determination of UT1. Earth Planets Space 62(12):933–937. doi:10.5047/eps.2010.11.008

Kareinen N, Hobiger T, Haas R (2015) Automated analysis of Kokee–Wettzell Intensive VLBI sessions—algorithms, results, and recommendations. Earth Planets Space 67:181. doi:10.1186/s40623-015-0340-x

Leek J, Artz T, Nothnagel A (2015) Optimized scheduling of VLBI UT1 intensive sessions for twin telescopes employing impact factor analysis. J Geod 89(9):911–924. doi:10.1007/s00190-015-0823-3

Lovell J, McCallum J, Shabala S, Plank L, Böhm J, Mayer D, Sun J (2014) Dynamic observing in the VGOS era. In: Baver KD, Behrend D, Armstrong KL (eds) IVS 2014 general meeting proceedings "VGOS: The New VLBI Network". Science Press, Beijing, pp 43–47

Malkin Z (2013) Impact of seasonal station motions on VLBI UT1 intensives results. J Geod 87(6):505–514. doi:10.1007/s00190-013-0624-5

Nilsson T, Haas R (2010) Impact of atmospheric turbulence on geodetic very long baseline interferometry. J Geophys Res Sol Ea 115(B3): b03407. doi:10.1029/2009JB006579

Nothnagel A, Artz T, Behrend D, Malkin Z (2016) International VLBI service for geodesy and astrometry—delivering high-quality products and embarking on observations of the next generation. J Geod. doi:10.1007/s00190-016-0950-5

Otsubo T, Matsuo K, Aoyama Y, Yamamoto K, Hobiger T, Kubo-oka T, Sekido M (2016) Effective expansion of satellite laser ranging network to improve global geodetic parameters. Earth Planets Space 68(1):65. doi:10.1186/s40623-016-0447-8

Petit G, Luzum B (eds) (2010) IERS conventions (2010). IERS technical note 36, Verlag des Bundesamts für Kartographie und Geodäsie, Frankfurt am Main

Petrachenko B, Niell A, Behrend D, Corey B, Böhm J, Charlot P, Collioud A, Gipson J, Haas R, Hobiger T, Koyama Y, MacMillan D, Malkin Z, Nilsson T, Pany A, Tuccari G, Whitney A, Wresnik J (2009) Design aspects of the VLBI2010 system. Progress report of the IVS VLBI2010 committee

Plag HP, Pearlman M (eds) (2009) Global geodetic observing system: meeting the requirements of a global society on a changing planet in 2020. Springer, Berlin

Sovers OJ, Fanselow JL, Jacobs CS (1998) Astrometry and geodesy with radio interferometry: experiments, models, results. Rev Mod Phys 70(4):1393–1454. doi:10.1103/RevModPhys.70.1393

Treuhaft RN, Lanyi GE (1987) The effect of the dynamic wet troposphere on radio interferometric measurements. Radio Sci 22(2):251–265. doi:10.1029/RS022i002p00251

Uunila M, Nothnagel A, Leek J (2012) Influence of source constellations on UT1 derived from IVS INT1 sessions. In: Behrend D, Baver KD (eds) IVS 2012 general meeting proceedings "Launching the Next-Generation IVS Network", NASA/CP-2012-217504, pp 395–399

Wessel P (2009) A general-purpose Green's function-based interpolator. Comput Geosci 35(6):1247–1254. doi:10.1016/j.cageo.2008.08.012

Wessel P, Smith WHF, Scharroo R, Luis J, Wobbe F (2013) Generic mapping tools: improved version released. EOS Trans AGU 94(45):409–410. doi:10.1002/2013EO450001

Whitney A, Lonsdale C, Himwich E, Vandenberg N, van Langevelde H, Mujunen A, Walker C (2002) VEX file definition/example. http://www.vlbi.org/vex/docs/vex%20definition%2015b1.pdf, technical report 1.5b1. Accessed 5 Jan 2017

Submit your manuscript to a SpringerOpen journal and benefit from:

- ► Convenient online submission
- ► Rigorous peer review
- ► Immediate publication on acceptance
- ► Open access: articles freely available online
- ► High visibility within the field
- ► Retaining the copyright to your article

Submit your next manuscript at ► springeropen.com